

Short Communication

# Electropolymerization of Pyrrole and Electrochemical Study of Polypyrrole 4. Electrochemical Oxidation of Non-Conjugated Pyrrole Oligomers

Ming Zhou,<sup>†</sup> Volker Rang and Jürgen Heinze\*

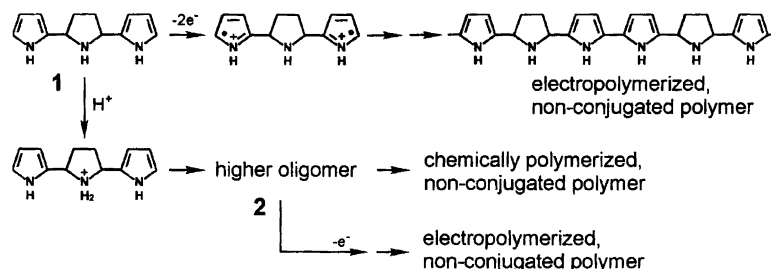
Institut für Physikalische Chemie, Albertstrasse 21, Freiburger Materialforschungszentrum, Stefan-Meier-Str. 21, Albert-Ludwigs-Universität Freiburg, D-79104 Freiburg, Germany

**Dedicated to Professor Henning Lund on the occasion of his 70th birthday.**

Zhou, M., Rang, V. and Heinze, J., 1999. Electropolymerization of Pyrrole and Electrochemical Study of Polypyrrole 4. Electrochemical Oxidation of Non-Conjugated Pyrrole Oligomers. – Acta Chem. Scand. 53: 1059–1062. © Acta Chemica Scandinavica 1999.

The electropolymerization of pyrrole and the properties of polypyrrole (PPy) have been described in numerous publications. Nevertheless, many questions concerning the mechanism of electropolymerization remain open. In our multi-part account relating to the electropolymerization of pyrrole, we have reported a structural diversity<sup>1</sup> of PPy and accordingly, proposed a multi-pathway mechanism<sup>2</sup> for the formation of different PPy variants, which we called PPy(I), PPy(II) and PPy(III) (Fig. 1). Because two protons are released in each coupling step during polymerization, we have suggested that, as a side reaction, the proton-catalyzed trimerization<sup>3–5</sup> of pyrrole, leading to 2,2'-(2,5-pyrroli-dinediyl)dipyrrole (**1** in Scheme 1), and a successive electrochemical polymerization of **1**, leading to an isolating film,<sup>2</sup> play a significant role in the overall electropolymerization of

pyrrole in acetonitrile. From this point of view, some issues, such as the shapes of voltammograms and the long controversial 'water effect',<sup>6–14</sup> can be better interpreted. The broad and symmetric voltammograms of PPy, which are normally found when electropolymerization occurs at a high rate and, consequently, the reaction layer in the vicinity of the electrode becomes acidic, can be attributed to an electrochemically generated copolymer PPy(III) from **1** and pyrrole. Water, as a fairly strong base in acetonitrile,<sup>15</sup> captures the protons released from coupling reactions and prevents pyrrole molecules from undergoing acid-catalyzed trimerization and subsequent oligomerization.<sup>16</sup> In order to substantiate the mechanism proposed in the previous papers,<sup>2,16</sup> we report here for the first time the electrochemical oxidation of **1** and its copolymerization with pyrrole.



Scheme 1. Formation of the non-conductive layer from 2,2'-(2,5-pyrroli-dinediyl)dipyrrole **1**.

<sup>†</sup> Present address: Institute for Chemical Process and Environmental Technology, National Research Council Canada, Montreal Road, Ottawa, Ontario, Canada, K1A 0R6.

\* To whom correspondence should be addressed.

The results clearly show that **1**, as an intermediate during the polymerization of pyrrole in acidic acetonitrile, causes the formation of a passivation layer on the electrode.

Having employed a modification of Dennstedt's syn-

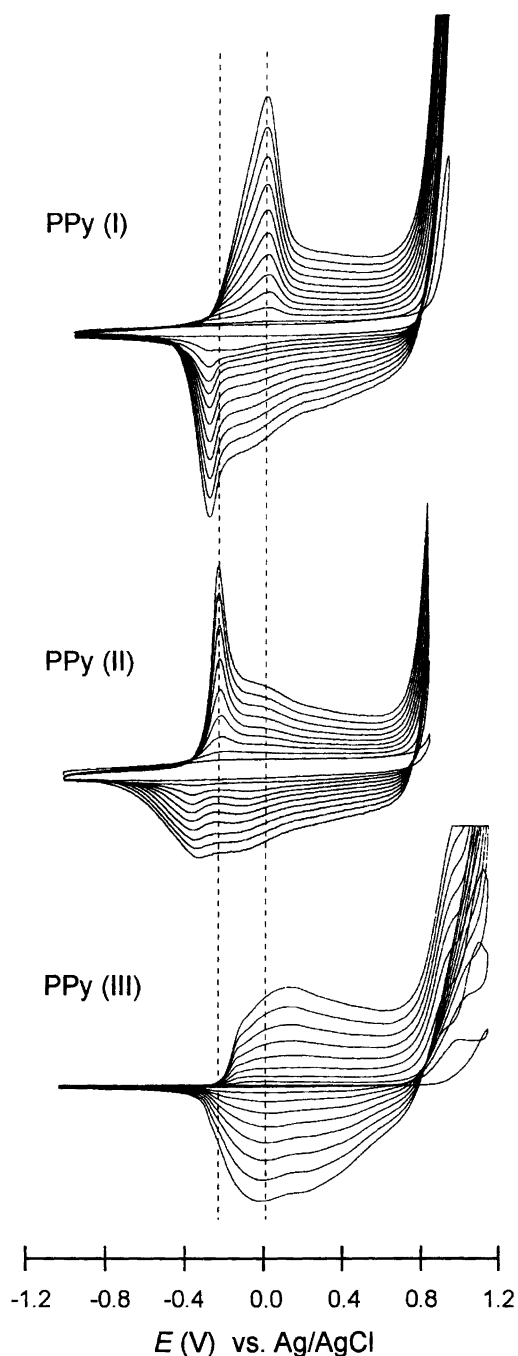


Fig. 1. Potentiodynamic formation of different PPy variants: PPy(I) with anodic peak at 0.0 V is formed under normal mild conditions in neutral acetonitrile; PPy(II) with anodic peak at  $-0.23$  V is formed at very low reaction rates in weakly acidic acetonitrile; PPy(III) with symmetric voltammograms is formed at high reaction rate or in acidic acetonitrile.

thesis procedure,<sup>5,17,18</sup> we isolated both **1** (purified by sublimation) and a red, structurally unknown oligomer (**2** in Scheme 1), which is only slightly soluble in water but has good solubility in acetonitrile. The cyclic voltammograms of both **1** and **2** were recorded with the solutions indicated in the figure captions.

Cyclic voltammograms of **1** in dried acetonitrile are

shown in Fig. 2. When the potential scan was applied from  $-1.22$  V to any switching potential at which the oxidation of **1** took place, we observed strong electrode passivation, which is manifested by the current drop with increasing scan number. When the switching potential was changed to more positive values (from 0.78 V in Fig. 2A to 1.18 V in Fig. 2C), the current drop between two consecutive scans increased, indicating faster passivation at higher potentials. In addition, neither the characteristic 'nucleation loop'<sup>1,8</sup> nor electroactive deposit could be seen in any cycle at any potential range. This unequivocally confirms that electro-oxidation of **1** results in the formation of a non-conductive layer on the electrode. As for the peak potential  $E_{pa}$ , the value of ca. 0.95 V, as indicated in Fig. 2C, is not an exact measurement, because the electrode passivation produces a negative shift of the peak position. However, it is clear that the oxidation of **1** and the subsequent electrode passivation already take place at potentials much lower than 0.78 V (Fig. 2A). By comparison, apparent electro-oxidation of pyrrole (in a solution of 0.1 M pyrrole) starts at potentials higher than 0.8 V.

The addition of pyrrole (0.1 M) and water ( $5.5 \times 10^{-3}$  M) to the above solution of **1** did not significantly change the voltammetric response. Figures 2D–F, obtained with the solution containing water and pyrrole, demonstrate the same electrode passivation as that in Figs. 2A–C. This situation is quite similar to the results obtained from highly acidified acetonitrile solution (see Fig. 2 in the previous paper<sup>2</sup>), in which there was a high concentration of **1** formed via acid-catalysed reactions. Even very high concentrations of pyrrole (0.5 M) did not produce any conductive polymer. The concentration ( $3.7 \times 10^{-3}$  M) of **1** must be too high, thus strongly passivating the electrode before the oxidation of pyrrole. In solutions containing only  $1 \times 10^{-3}$  M of **1**, the observed anodic current, up to a switching potential of 0.95 V, results mainly from the oxidation of **1** (Fig. 3A). When the switching potential was raised to 1.11 V, following the shoulder on the first forward potential scan (mainly resulting from the oxidation of **1**), a steep increase in the anodic current was observed, owing to the oxidation of pyrrole, and a trace-crossing appeared upon scan reversal. However, the electrode passivation still governed the electrochemical processes, and the continuous growth of a conducting film was suppressed (Fig. 3B). As expected, continuous electropolymerization started at even higher switching potentials (1.17 V in Fig. 3C), at which pyrrole was predominantly oxidized. Showing broad and symmetric redox waves, the polymer formed in Fig. 3C is a partially conjugated copolymer PPy(III).<sup>2</sup> Decreasing the concentration of **1** further, to ca.  $5 \times 10^{-4}$  M for example, can produce polymer at a switching potential ca. 1.0 V, and the CV of the polymer shows a shape somewhere between Fig. 3C and that of PPy(I). The key factor governing polymer growth or electrode passivation here is the ratio  $[I^{(2)'+}]/[Py^+]$ . Interestingly, because the oxidation of **1** precedes the

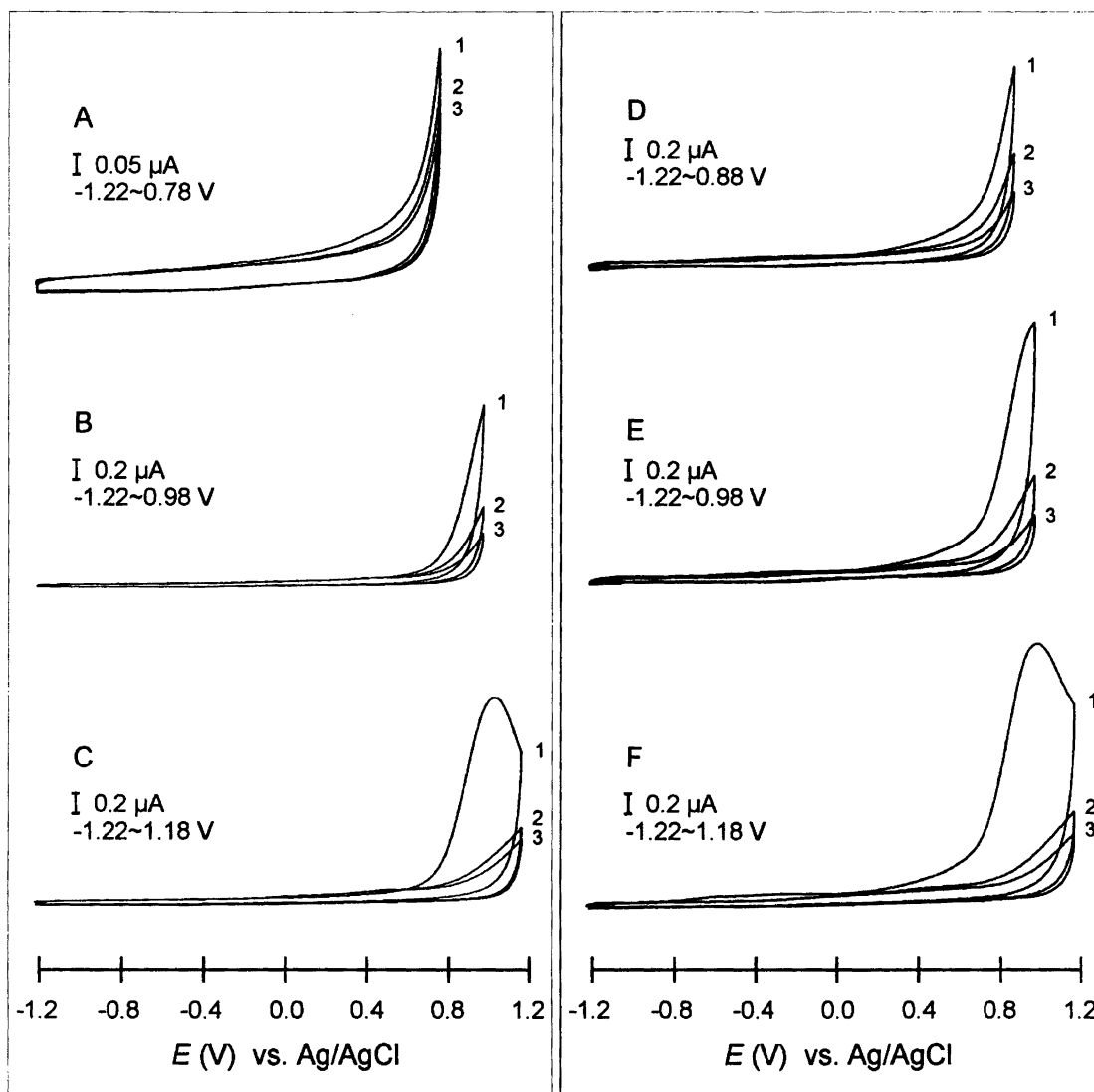


Fig. 2. Electrode passivation upon electrochemical oxidation of **1** ( $3.7 \times 10^{-3}$  M) in acetonitrile–0.1 M TBAPF<sub>6</sub>,  $T = 253$  K, scan rate  $0.1$  V s<sup>-1</sup>: (A)–(C) in the absence of pyrrole and water; (D)–(F) containing 0.1 M pyrrole and  $5.5 \times 10^{-3}$  M water.

oxidation of pyrrole during each forward potential scan, and the electrode thus becomes less active before the steep current increase from pyrrole oxidation, the trace-crossing ('nucleation loop') of the forward and backward scans<sup>1,8</sup> can be observed not only in the first cycle, but also in several following potential cycles.

In our discussion on the mechanism of **1**-related side reactions, it was also mentioned<sup>2</sup> that, in addition to **1**, other higher, but ill-defined oligomers, which can take any structure during the course of chemical polymerization of **1**, might undergo a similar electrochemical oxidative coupling path leading to the formation of a non-conjugated polymer. Voltammetric investigation of **2** demonstrates the same facts, i.e., the electro-oxidation of **2** begins to occur at potentials lower than 0.8 V, and the electrode passivation is the only observed event upon electrochemical oxidation of **2**. In conclusion, the results

from both **1** and **2** are the cornerstone for the mechanism suggested in the previous papers in this series.

### Experimental

**Synthesis of 1 and 2.** Pyrrole (Aldrich) was distilled under argon immediately before use. Hydrochloric acid was diluted to 6 M and ammonia water diluted to 3 M. The chemical synthesis procedure is as described in Ref. 5. Hydrochloric acid (40 ml, 0.24 mol) was placed in a 500 ml three-necked flask fitted with two constant-pressure addition funnels, gas inlet, and a magnetic stirrer. Pyrrole (10 ml, 0.14 mol) and ammonia (90 ml, 0.27 mol) were placed in the two funnels. The system was purged and filled with argon after which the flask was cooled to 0 °C and pyrrole was quickly added with vigorous stirring. After 30 s the reaction was quenched

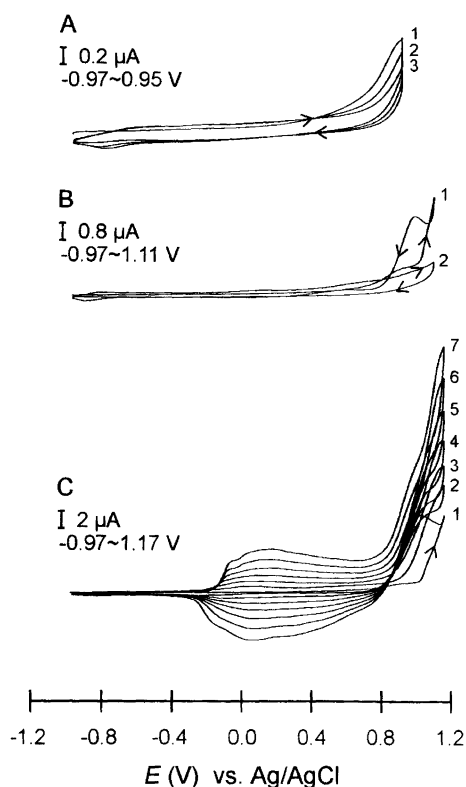


Fig. 3. Co-oxidation and copolymerization of **1** and pyrrole in acetonitrile–0.1 M TBAPF<sub>6</sub>,  $1 \times 10^{-3}$  M **1**, 0.1 M pyrrole and  $5.5 \times 10^{-3}$  M water.  $T = 253$  K, scan rate  $0.1$  V s<sup>-1</sup>.

with the ammonia solution. The mixture, containing an oily substance and a red solid **2**, was diluted with 100 ml of water (0°C) and filtered. The filtrate was then extracted with 150 ml of ether. The ether solution was evaporated under reduced pressure, and light yellow substance was obtained with a yield of 32% (3.07 g). Purification by sublimation produced a white solid **1**. Compound **2** was washed with water and dissolved in ether. After evaporation of ether, sponge-like **2** was left in the flask. Analysis of **1**: m.p. 89–96°C (Ref. 5: 86–90°C). UV–VIS (*n*-hexane):  $\lambda_{\text{max}} = 212$  nm. Anal. Calc. for C<sub>12</sub>H<sub>15</sub>N<sub>3</sub>: C, 71.61%; H, 7.51%; N, 20.88%. Found: C, 71.82%; H, 7.23%; N, 21.07%. MS (70 eV), *m/z* (%): 201 (49.5), 184 (100). <sup>1</sup>H NMR (300 MHz, CDCl<sub>3</sub>):  $\delta$  2.0, 2.2 (m, 4 H, CH<sub>2</sub>), 2.2 (s, 1 H, NH pyrrolidine unit), 4.2, 4.3 (t, 2 H, CH pyrrolidine unit), 6.0 (d, 2 H, =CH– pyrrole unit), 6.1 (t, 2 H, =CH– pyrrole unit), 6.6 (d, 2 H, =CH– pyrrole unit), 8.7 (d, 2 H, NH pyrrole unit); all chemical shifts were referenced to CHCl<sub>3</sub> ( $\delta$  7.24). <sup>13</sup>C NMR (75 MHz, CDCl<sub>3</sub>):  $\delta$  32.36, 32.43 (CH<sub>2</sub> pyrrolidine unit), 55.09, 54.99 (CH pyrrole unit), 104.16, 104.33 (=CH– pyrrole unit), 108.10, 108.16 (=CH– pyrrole unit), 116.94, 117.04 (=CH– pyrrole unit), 134.18, 134.41 (=CH– pyrrole unit); all chemical shifts were referenced to CDCl<sub>3</sub> ( $\delta$  77.00). All peaks appeared as pairs due to the isomerism of the molecule. The

analysis is consistent with the structure of **1** in Scheme 1 and with the data given in Ref. 5.

**Electrochemical measurement.** Tetrabutylammonium hexafluorophosphate (TBAPF<sub>6</sub>, Fluka, electrochemical grade) was used as received. Commercial HPLC grade acetonitrile (Fisons Scientific Equipment) was distilled from CaH<sub>2</sub> under argon before use. The cyclic voltammetric experiments were conducted in a three-electrode cell under argon. A Pt disk (diameter 1 mm, area 0.785 mm<sup>2</sup>) sealed in a soft glass rod was employed as the working electrode. Pt and Ag wires were used as counter- and quasi-reference electrodes, respectively. Potentials versus the Ag quasi-reference electrode were then rescaled by Ag/AgCl, calibrated with the ferrocene/ferrocenium redox couple (0.35 V vs. Ag/AgCl). An EG & G Potentiostat/Galvanostat Model 273 and a Kipp & Zonen Delft BV BD 92 recorder were used for electrochemical control and data recording, respectively.

**Acknowledgements.** Dr. Ming Zhou is grateful to the Alexander von Humboldt Foundation for an Alexander von Humboldt Research Fellowship. Financial support from the DFG and the *Fonds der Chemischen Industrie* is gratefully acknowledged.

## References

- Zhou, M. and Heinze, J. *Electrochim. Acta* 24 (1999) 1733.
- Zhou, M. and Heinze, J. *J. Phys. Chem., Part 2. In press.*
- Potts, H. A. and Smith, G. F. *J. Chem. Soc.* (1957) 4018.
- Smith, G. F. *Adv. Heterocycl. Chem.* 2 (1963) 287.
- Lamb, B. S. and Kovacic, P. *J. Polym. Sci., Polym. Chem. Ed.* 18 (1980) 1759.
- Diaz, A. F., Kanazawa, K. K. and Gardini, G. P. *J. Chem. Soc., Chem. Commun.* (1979) 635.
- Kanazawa, K. K., Diaz, A. F., Gill, W. D., Grant, P. M., Street, G. B., Gardini, G. P. and Kwak, J. F. *Synth. Met.* 1 (1979/80) 329.
- Downard, A. J. and Pletcher, D. *J. Electroanal. Chem.* 206 (1986) 139.
- Heinze, J., Hinkelmann, K. and Land, M. *DECHEMA Monographie* 112 (1988) 75.
- Heinze, J. *Top. Curr. Chem.* 152 (1990) 1.
- Beck, F., Oberst, M. and Jansen, R. *Electrochim. Acta* 35 (1990) 1841.
- Beck, F. *Electrochim. Acta* 33 (1988) 839.
- Zotti, G., Schiavon, G., Berlin, A. and Pagani, G. *Electrochim. Acta* 34 (1989) 881.
- Otero, T. F. and Rodriguez, J. *J. Electroanal. Chem.* 379 (1994) 513.
- Kolthoff, I. M. and Ikeda, S. *J. Phys. Chem.* 65 (1961) 1020.
- Further evidences supporting our explanation of a 'water effect' and a comprehensive review of existing speculations were given in Part 3. *J. Phys. Chem. In press.*
- Dennstedt, M. and Zimmermann, J. *Ber. Deutsch. Chem. Ges.* 21 (1888) 1478.
- Dennstedt, M. and Voigtländer, F. *Ber. Deutsch. Chem. Ges.* 27 (1894) 476.

Received January 11, 1999.